MCDONNELL DOUGLAS
CORPORATION

1. Report No.	2. Government Accession No.	3. Recipient's Catalog No.
NASA CR-159732		

4. Title and Subtitle
AMPLIFICATION OF REYNOLDS NUMBER DEPENDENT PROCESSES BY WAVE DISTORTION

5. Report Date
November 1979

6. Performing Organization Code

7. Author(s)
M. Ventrice

8. Performing Organization Report No.

10. Work Unit No.

9. Performing Organization Name and Address
Department of Mechanical Engineering
Tennessee Technological University
Cookeville, Tennessee 38501

11. Contract or Grant No.
NGR 43-003-015

13. Type of Report and Period Covered
Final Report
Jan. 1, 1972-Oct. 31, 1979

12. Sponsoring Agency Name and Address
National Aeronautics and Space Administration
Washington, D.C. 20546

14. Sponsoring Agency Code

15. Supplementary Notes
Richard J. Priem, Technical Monitor
NASA Lewis Research Center
Cleveland, Ohio

16. Abstract

The object of the research was t ynolds number dependent process by wave distortion esults to other similar Reynolds number dependent pr as that associated with the operation of a constant-tempe plication of most interest was investigation of vaporizat ustion typcially associated with liquid propellant rocke

A series of experiments were car ive distortion on a Reynolds number dependent process the anemometer process and the combustion process. lies were involved, both having the ultimate objective of zing behavior common to different chamber geometries and d

The results indicate a high degr sses and the possibility of using the anemometer sy ility. The nonlinear aspects of a Reynolds numb he dominant mechanisms controlling instability.

17. Key Words (Suggested by Author(s))
Combustion instability
Liquid fuel combustion

19. Security Classif. (of this report)	20. Sec	f Pages	22. Price*
Unclassified (U)	Un		

* For sale by the National Te 2161

FOREWORD

The research summarized in this report was carried out by a number of individuals who functioned in various capacities. The initial idea for the research originated with Allan E. Hribar, who was also the first principal investigator. Later, Kenneth R. Purdy and finally Marie B. Ventrice served as principal investigators. There have also been several faculty associates: John P. Wallace, Kenneth R. Purdy, Marie B. Ventrice, and John Peddieson, Jr.. The Ph.D. level graduate students who participated were Marie B. Ventrice, Jih-Chin Fang, and Kin-Wing Wong. The masters level students were John Bordenet, Jr. and Gary H. McDonald and A. Googerdy.

The advice, encouragement, and support of Richard J. Priem, the technical monitor for the research, has been very important and is gratefully acknowledged and appreciated.

Critical support was provided by Tennessee Technological University through the Department of Mechanical Engineering. In addition, the cooperation of the Department of Engineering Science and Mechanics played an important role in the research.

TABLE OF CONTENTS

Introduction and Background

The object of this report is to summarize the research and the significant results of the research which was carried out under NASA Grant NGR 43-003-015 from January 1, 1972, until the grant termination on October 31, 1979.

The purpose of the research was to study high-frequency combustion instability in liquid-fuel rocket engines--instability in which the combustion process is coupled to acoustic waves. To do this, new experimental and analytical tools and techniques were developed. Basically, it was desired to develop a better understanding of and more insight into the fundamental phenomena associated with combustion instability, with the view that results of such studies would not be confirmed in application to liquid-fuel combustor instability, (a Reynolds Number dependent process), but would have general application to other Reynolds Number dependent processes. These other processes would include those associated with all types of combusters--solid- as well as liquid-fuel rocket engines, jet engines, and furnaces.

Combustion instability has been a persistant problem in both liquid- and solid-fuel rocket-engine development programs. In liquid-fuel rocket engines, the fuel and oxydizer are injected into the combustion chamber where they are vaporized and combustion takes place. The resulting hot gases continue through the chamber and are accelerated to supersonic velocities by means of a converging-diverging nozzle and ultimately leave the engine. This process is not smooth, but has associated with it background oscillations which are detected as fluctuations in gasdynamic variables such as pressure, density, temperature, and so forth. (These oscillations can be a result of a number of phenomena such as turbulence

In addition, some initial minimum amplitude of gasdynamic disturbance was necessary to excite instability.

Analytically, some success had been achieved with modeling. It was generally accepted that combustion instability was primarily sensitive to fluctuations in the gas pressure and the velocity of the fuel drops relative to the gas. The problem of pressure-sensitive combustion instability had a long history of successful analytical treatment; but, because of its greater mathematical complexity, much less work had been done with analysis of velocity-sensitive combustion instability.

Acquiring the understanding of combustion instability needed to formulate rational design procedures depended critically on the development of realistic modeling techniques, and it was toward this end that this research was begun. Initially the emphasis was on development of an experimental analog of the combustion-acoustics interaction. Later, analytical techniques were developed, partially in support of the experimental work and partially as a valuable study in its own right.

Several specific observations led to the initiation of this research. First Priem [1] established a model in which combustion is viewed as vaporization-limited (i.e., as a velocity-sensitive or Reynolds number dependent process). Later, Heidman [2, 3] showed that distorted acoustic oscillations (fundamental frequency oscillations plus high harmonic "distortion") affect the open-loop response of this vaporization-limited combustion. The response is a measure of the degree of reinforcement of the acoustic oscillations and the combustion process. It is important to know how the instantaneous gasdynamic acoustic field combines with the acoustic field resulting from the combustion process. One of the better ways of relating these two fields is to find the correlation between the pressures of each. Such a correlation could then be used to determine the

closed-loop response. But no explicit expression for the acoustic pressure which results from a particular combustion process was available; hence, Heidmann analytically compared the existing pressure with the burning rate of the combustion process, i.e., he formed an open-loop response. He used harmonic response factors to indicate the degree of reinforcement of the acoustic pressure by the combustion process and found that the response factors depended upon the amplitudes of the harmonic components and the phase between the acoustic pressure and burning rate harmonic components. Lastly, Hribar [4] noticed the similarity of the open-loop responses of a liquid-fuel droplet's vaporization rate and a constant-temperature hot-wire anemometer's energy transfer rate to the same gasdynamic environment.

Combining the above observations, Hribar [4] proposed the development of an analog technique for studying combustion instability, in which a constant-temperature hot-wire anemometer would serve as the analog to combustion. The advantages to such a system would be many. The analog would not involve an actual combustion process so that the many problems associated with making measurements in a hot, burning mixture would be avoided. The system could be more easily controlled; studies could be done with the analog which would not be possible using an actual combustion situation. (For example, parameters could be varied independently, a feature not possible in an actual combustion situation.) Also, the analog technique would be less expensive than actual experimental combustion studies.

Because of the above, the initial objective of the research was to develop an analog system for the study of combustion instabilities in liquid-propellant rocket engines, and then to use the analog to investigate the basic mechanisms governing these instabilities. Later, the research was expanded to include mathematical analysis techniques, initially to determine

whether or not certain effects that were observed experimentally with the analog could be predicted mathematically. These analytical studies resulted in improved insight into analytical modeling techniques.

What follows in this report is a chronological description of the research and the significant results. Most of what was done has been documented in various papers, theses, and dissertations. Hence, specific details of the research will be kept to a minimum and the appropriate references will be mentioned in which more detailed descriptions can be found.

Research

As was stated earlier, the initial objective of the research was to develop an analog system for the study of high frequency combustion instabilities in liquid-propellant rocket combustion chambers. Before considering the analog, an understanding of the phenomena being modeled is necessary.

Combustion Model. To characterize the combustion process, the combustion model due to Priem [1], in which the combustion is viewed as vaporization-limited, was used. In this model the burning rate is equal to the vaporization rate of the liquid propellant droplets, and this vaporization or burning rate W is given as

$$W = C_1 + C_2 \, Re^{0.5} \tag{1a}$$

where

$$C_1 = \frac{2\pi D M_\ell \mathcal{D}_d}{R_u T} P \ln \frac{P}{P-P_v} \tag{1b}$$

$$C_2 = \frac{0.6 \, Sc^{0.33} \pi D M_\ell \mathcal{D} C_d}{R_u T} P \ln \frac{P}{P-P_v} \tag{1c}$$

and

$$Re = \frac{\rho D \, |\vec{V} - \vec{V}_d|}{\mu} \tag{1d}$$

where D is the inside diameter of the combustion chamber, M_ℓ is the molecular weight of the propellant, $\mathcal{D}$ is the molecular diffusion coefficient, C_d is the concentration of propellant drops, R_u is the universal gas constant, T is the gas temperature, P is the gas pressure, P_v is the vapor pressure of the fuel, S_c is the Schmidt number, ρ is the gas density, $\vec{V}$ is the gas velocity, $\vec{V}_d$ is the propellant droplet velocity and μ is the dynamic viscosity. Equations (1) indicate that the vaporization rate is convection limited (Reynolds number dependent) with additional sensitivity to the gasdynamic and droplet variables.

In Priem's model, the burning rate is sensitive to the magnitude of the surrounding gas velocity with respect to the drop velocity, i.e., it is sensitive to a "rectified" relative velocity. This causes higher harmonic frequency components of the burning rate to occur in response to fundamental frequency perturbations of the gasdynamic field. In addition to this method of generating higher harmonic components of the burning rate, and consequently of the gasdynamic variables, nonlinear gasdynamic effects will also generate higher harmonic components of the gasdynamic variables.

As was mentioned earlier, during combustion in liquid-propellant rocket engines, the combustion process and the gasdynamic processes are coupled. Any oscillation in gasdynamic variables causes an oscillatory burning rate; and the oscillatory burning process serves as the energy source to sustain gas dynamic oscillations. Under certain conditions, when the energy supplied by an unsteady combustion process is sufficient to overcome the energy losses in the gasdynamic field, the coupling is self-sustained and the oscillations can build to large amplitudes, a condition referred to as unstable combustion.

The Analog. The analog selected to model the vaporization-limited combustion process was a hot-wire sensor and the associated series output of a constant temperature hot-wire anemometer, a phase change or time delay device, a power amplifier, and an acoustic driver. The heart of the analog is the anemometer which applies a voltage across the hot-wire, causing it to heat to some preset temperature (resistance) level. Any flow which passes over the wire tends to cool it, but the anemometer responds to counteract this by increasing the voltage across the wire. The bridge voltage of the anemometer E is related to the flow over the wire. This relationship can be expressed as

$$E^2 = \frac{[R_w + R_{cbl} + R_p + R_s]^2}{R_w} [C_3 + C_4 \, Re_f^m] \qquad (2a)$$

where

$$C_3 = \pi L_w k_f \left[T_f/T\right]^{0.17} \left[T_w - T\right]A \tag{2b}$$

$$C_4 = \pi L_w k_f \left[T_f/T\right]^{0.17} \left[T_w - T\right]B \tag{2c}$$

and

$$Re_f = \frac{\rho_f D_w |\vec{V}|}{\mu_f} \tag{2d}$$

where D_w is the diameter of the hot-wire, R_w is the operating resistance of the hot-wire, R_{cbl} is the resistance of the cable connecting the hot-wire and probe to the anemometer, R_p is the probe resistance, R_s is the appropriate anemometer resistance, m, A, and B, are coefficients whose exact values are determined by calibration of the individual hot-wire (typical values are m = 0.4442, A = 0.5205 and B = 0.6729; details on hot-wire calibration can be found in [5], [6], [7], [8], L_w is the length of the hot-wire, k_f is the gas (air) thermal conductivity evaluated at the film temperature $T_f = [T + T_w]/2$, T is the gas temperature, T_w is the hot-wire operating temperature, ρ_f is the gas density evaluated at the film temperature, V is the component of the gas velocity normal to the stationary hot-wire and μ_f is the dynamic viscosity evaluated at the film temperature. (Discussions of the development of Equations (2) are given in several references by Purdy, Ventrice, and Fang [5, 6, 8, 9].) Equations (2) indicate that the square of the anemometer output voltage is analogous to the convection limited burning rate $\dot{W}$ given by Equations (1). To complete the analogy, a phase change or time delay device is used as the analog of the phase change or time delay associated with combustion, a power amplifier is used as the analog of the energy released during the burning of the propellant, and an acoustic driver is used to convert the energy associated with the anemometer and power amplifier to gasdynamic energy.

In the analog model, the anemometer output is dependent upon the magnitude of the gas velocity normal to the hot-wire, i.e., it is sensitive to a "rectified" relative velocity. As in combustion, this causes higher harmonic frequency components of the anemometer output to occur in response to fundamental frequency oscillations in the gas velocity field. In addition to the nonlinearity of the analog process resulting in higher harmonic components of the anemometer output voltage, and consequently of the gasdynamic variables, nonlinear gasdynamic effects also generate higher harmonic perturbations of the gasdynamic variables.

A series of events, analogous to those which occur in the combustion system, occur in the analog system. Acoustic perturbations in the gasdynamic field are sensed by the hot-wire. The resulting anemometer output signal is amplified, after phase change or time delay, and fed to the acoustic driver, which generates gasdynamic perturbations proportional to the signal to it. These new acoustic perturbations combine with the previous ones to form a new gasdynamic field. As in combustion, in some situations the perturbations will reinforce each other and be sustained or increased in intensity; in other cases they will die out.

A comment needs to be made concerning the anemometer output signal mentioned above. The anemometer actually has two output signals--E, the bridge voltage and E', the time-dependent or fluctuating component of the bridge voltage, where $E = \bar{E} + E'$. (The component $\bar{E}$ is the time-mean component.) It is E^2 which is analogous to the burning rate W and E^2 also has a time-mean and a fluctuating component, i.e., $E^2 = (\overline{E^2}) + (E^2)'$. (The bar over a property is used to indicate the time-mean component and the prime designates the time-dependent component.)

From the above it can be seen that $E^2 = \bar{E}^2 + 2\bar{E}E' + (E')^2 = (\overline{E^2}) + (E^2)'$. Only the fluctuating component of E^2 would drive acoustic oscillations;

hence, $(E^2)'$ would be the required signal to be used in the analog system. However, when E' is small relative to $\bar{E}$ (which is the case for the analog system), Fang [8] has shown that E' characterizes $(E^2)'$ to a satisfactory degree with respect to amplitudes, frequencies, and phases. Hence, E' was used as the feedback signal in the loop.

Initial Research Plan. At the outset of the research, the above description of the analog had not been fully conceptualized and the validity of the description had not been established. As the research progressed, the above description evolved.

To initiate the analog studies, the following was proposed.

1. To analytically perform an open-loop response factor analysis of the analog to see if the same results would be obtained as Heidmann obtained for vaporization-limited combustion. For these studies the pressure associated with an acoustic field would be compared with the resulting anemometer output (analogous to the burning rate in combustion) and a response factor obtained. Various amounts and types of distortion would be added to determine stability predictions. This process would establish similarity between combustion and the analog.

2. If the results of the above were in agreement with Heidmann, to experimentally perform an open-loop analysis of the analog to determine if the analog would perform as predicted by theory.

3. To operate the analog system in the closed-loop mode to determine if the open-loop predictions of closed-loop behavior were valid. The above three items, if successful, would confirm the validity of Heidmann's analytical technique and the prediction that distorted acoustic waves would drive combustion, or the analog process, to instability. Once all of the above was accomplished, the analog system could then be used for further experiments designed to identify other factors important to unstable combustion.

Analytical Open-Loop Studies. The nonlinear, in-phase response factor developed and used by Heidmann is defined as

$$R_{n\ell} = \frac{\int_0^{2\pi} \tilde{w}' \, \tilde{p}' \, d(\omega t)}{\int_0^{2\pi} (\tilde{p}')^2 \, d(\omega t)}$$

where $\tilde{w}'$ is the time-dependent, dimensionless perturbation in the normalized burning rate ($\tilde{w}' \equiv w'/\bar{w}$) and $\tilde{p}'$ is the time-dependent, dimensionless

perturbation in the pressure ($p = \bar{p} + p' = \bar{p}\,(1 + p'/\bar{p}) = \bar{p}\,(1 + \tilde{p}')$ where $\tilde{p}' \equiv p'/\bar{p}$).

The nonlinear, in-phase response factor used for the analog analysis is defined as

$$R_{n\ell} = \frac{\int_0^{2\pi} \tilde{E}'\,\tilde{p}'\,d\,(\omega t)}{\int_0^{2\pi} (\tilde{p}')^2\,d\,(\omega t)} \qquad (3)$$

where $\tilde{E}'$ is the time-dependent, dimensionless perturbation in the anemometer bridge voltage, i.e., $\tilde{E}' \equiv E'/\bar{E}$.

To obtain values for $R_{n\ell}$, the hot-wire's environment is specified. (As in Heidmann's work, the environment is considered to consist of a first tangential (1T) spinning resonant acoustic mode of vibration distorted by a second tangential (2T) spinning resonant acoustic mode of vibration. The relative magnitudes and phases can be varied.) This determines $\tilde{p}'$. Knowing the hot-wire's environment, and the calibration equation for the particular hot-wire being used, enables $\tilde{E}'$ to be determined. These can then be integrated, as in equation 3, to obtain $R_{n\ell}$.

The results obtained from the analytical open-loop studies of the analog process were qualitatively the same as those Heidmann obtained for vaporization-limited combustion. There were small differences in the actual numbers involved, but this was to be expected since the equations for the two processes were slightly different. A scaling factor would have been necessary to make a direct numerical comparison between the two. This was not done since only qualitative agreement was necessary.

The results showed that the addition of distortion to sinusoidal perturbations of the environment of the hot-wire could increase the response significantly. Using the stability criterion of Heidmann--response factors greater than some value between 0.8 and 1.0 denoted unstable operation (the oscillations would grow with time)--the analysis showed that certain

combinations of harmonic amplitude and phase angle would result in instability. The pure sinusoidal case was always predicted to be stable.

More detailed discussions of the analytical open-loop studies can be found in [5], [6], [9] and [11].

Experimental Open-Loop Studies. Since the analytical open-loop studies were successful, the experimental open-loop studies were carried out. The experimental technique for doing this was involved and is discussed in detail in [5] and [6].

A simplified schematic diagram of the experimental system used is shown in Figure 1. The object was to correlate an electrical signal, which was proportional to the fluctuations in the pressure of the acoustic field in the vicinity of the hot-wire, with the fluctuations in the anemometer output voltage and, from this, to calculate the response factor for that particular acoustic field. A variety of acoustic fields were used starting with an undistorted field at frequency f_{1T} and gradually adding to this distortion at $2f_{1T}$ so as to parallel the work done analytically.

To obtain response factors the system illustrated in the data acquisition system of Figure 1 was used. No instrument was available to directly determine a response factor so a response factor was calculated from the correlation coefficient R. Again, details of this can be found in [5] and [6].

The results of this aspect of the research were important in establishing the analog as a potential research tool. First of all, the experiments showed that it was possible to set up a physical system which could generate the same acoustic environment for a hot-wire probe that was investigated analytically and which could be used to determine the response of the hot-wire voltage to that environment. Secondly, the experimental results were qualitatively the same as the analytical results--the response

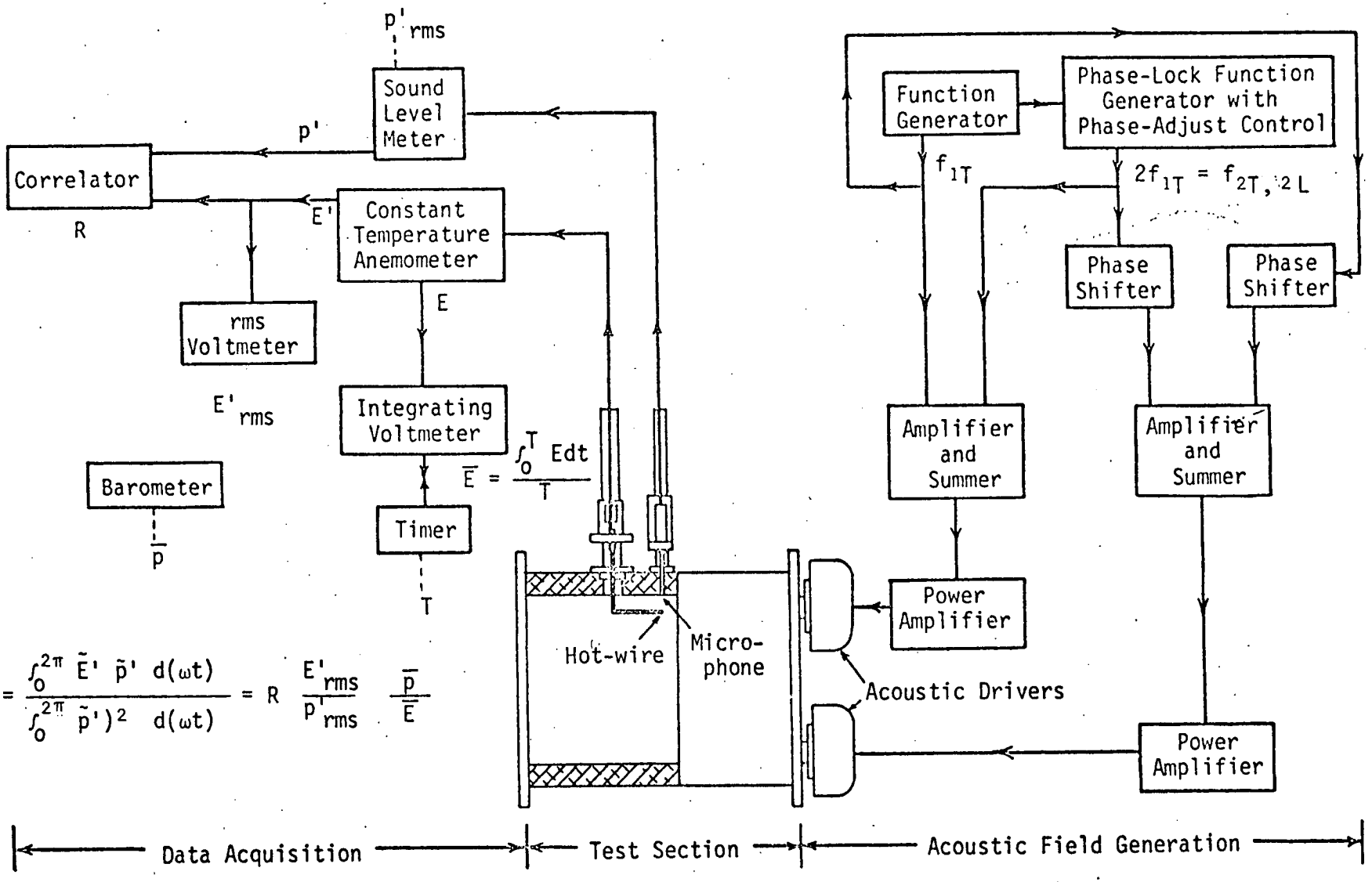

Figure 1. Schematic Diagram of the Open-Loop Experimental System

of the system to pure sinusoidal acoustic vibration was small, even when the magnitude of the acoustic pressure was large; the response could be increased by as much as an order of magnitude with respect to the sinusoidal case by the addition of distortion; and the amplitude and phase of the distortion component, relative to the fundamental component, were the dominant factors in the increase in the response.

Some problems did exist. The distorted acoustic fields could not be totally characterized by the equations resulting from the solution of the inviscid linear wave equation. Viscous effects should probably have been included in the analysis to account for acoustic streaming and any other secondary phenomena which might have been occurring. Also, there might have been some problems associated with the assumption used to obtain calibration constants for the hot-wire. The assumption was that the steady-state, steady-flow calibration of a hot-wire is applicable even when the wire is used in an unsteady situation.

Other discussions of the experimental open-loop investigations can be found in [5], [6], and [11].

Experimental Closed-Loop Studies. The closed-loop experimental studies posed many difficulties. Figure 2 is a very simplified schematic diagram of the experimental system. The test section's length-to-diameter ratio could be adjusted to two different values--one in which twice the frequency of the first tangential resonant mode of vibration was equal to the frequency of the second tangential-second longitudinal resonant mode of vibration, $2f_{1T} = f_{2T,\,2L}$; and one in which twice the frequency of the first tangential was not equal to a resonant frequency of the chamber, $2f_{1T} = f_x$. Two chambers were used to establish the effect of chamber dimensions on instability.

Referring to Figure 2, the gas-filled chamber could be excited by moving the switch into the upper position so that the function generator/amplifier

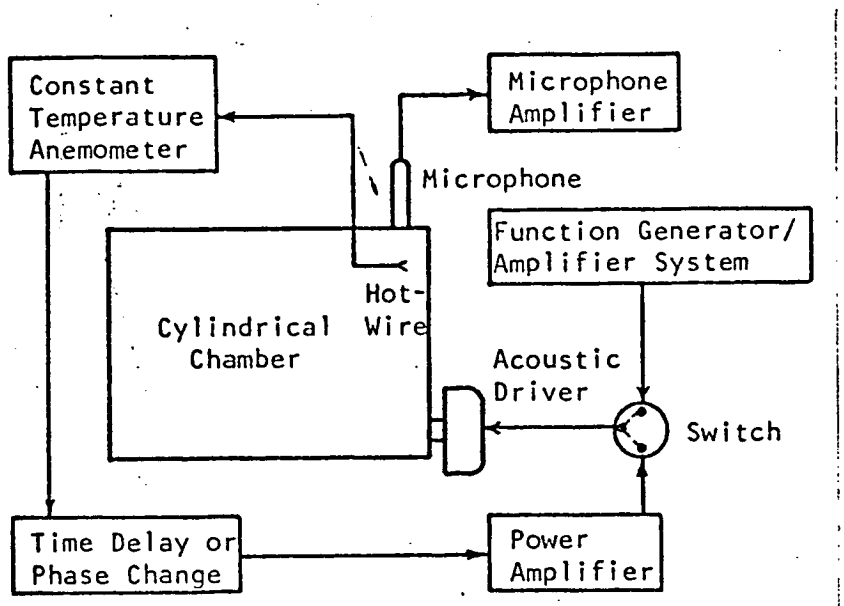

Figure 2. Simplified Schematic Diagram of the Closed-Loop Experimental System

system supplied the excitation signal to the driver (open-loop operation). By switching to its lower position, closed-loop operation could be obtained.

One objective of the closed-loop investigations was to confirm the results of the open-loop work, i.e., if the system was operating with a certain pattern of distorted acoustic oscillations, would it become unstable? This was not the only objective, however. Another objective was to allow the system to function over a wide range of variables and determine under what conditions instability developed and to determine if these conditions were consistent with those associated with unstable combustion and, from this, to perhaps gain insight into why these particular conditions develop.

To obtain a better understanding of closed-loop operation, the system was initially operated using a linear feedback device--the output of a microphone. This was a pressure-sensitive linear feedback process instead of the velocity-sensitive nonlinear feedback process of the anemometer analog system. Using the microphone, the characteristics of closed-loop system behavior at a single frequency could be studied and, ultimately, a

comparison could be made of pressure and velocity sensitive feedback processes and the pressure and velocity sensitivity of the combustion process.

A. Pressure-Sensitive Closed-Loop Experiments

Referring to Figure 2, the general procedure followed was to excite the chamber in the open-loop mode with some predetermined signal by means of the function generator/amplifier system. The switch was then moved to its alternate (closed-loop) operating position and the system was observed to see what would evolve. Three basic responses could develop: the acoustic pressure in the chamber could die out; the acoustic pressure could build in intensity to such a level that the switch had to be moved back to its open-loop position to avoid burning out the fuse in the driver circuit; or, finally, some type of steady-state acoustic pressure field could be attained. It was the conditions under which the third response occurred that were of interest. This represented a neutral stability situation. During the course of the experiments, several parameters were altered systematically to determine their effect on the closed-loop operation of the system. These were the open-loop signal from the function generator/amplifier system to the driver, the amount of time delay or amount of phase shift, the amount of amplification or gain, and the length-to-diameter ratio of the chamber.

The overall results of the linear feedback study were as follows:

1. The closed-loop sound field was independent of the character of the initial exciting sound field. The same closed-loop sound field resulted for a particular amount of gain and time delay or phase change in the loop, no matter what the characteristics of the initial open-loop sound field.

2. For a particular sound field to be self-sustained in closed-loop operation, the least amplification was required when the existing and

feedback sound fields were in phase with each other. If these two fields were not in phase with each other, more than this minimum feedback-loop amplification was required in order to have self-sustenance--the greater the phase difference between them, the greater the required feedback gain.

3. In general, the higher the gain, the higher the level of the closed-loop sound field. If self-sustenance did not occur at a certain phase difference between the existing and feedback field, increasing the gain or adjusting the phase difference so that the overall phase change through the loop was closer to a net zero would make the system self-sustaining.

4. Coexistence of two or more frequencies was possible whenever the gain was sufficient for each of them to be self-sustained. They were not normally integral multiples of each other.

5. None but resonant frequencies were self-sustaining.

6. The length-to-diameter ratio of the chamber did not effect the character of the results.

B. Velocity-Sensitive Closed-Loop Experiments

The general procedure followed was similar to that of the linear experiments--the chamber was excited in the open-loop mode with some predetermined signal by means of the function generator/amplifier system (see Figure 2). The switch was then moved to its closed-loop position and the system was observed to determine what type sound field would evolve.

The same three kinds of response could develop: the sound field could die out; the sound field could continuously build in intensity; or it could reach some steady-state operating level. The same parameters could be altered--the open-loop excitation signal, the time delay or phase shift, the gain, and the length-to-diameter ratio of the chamber.

It needs to be recalled here that the anemometer's response is non-linear--it is related to a "rectified" relative velocity. Because of this,

its output tends to be dominated by a component at 2f when exposed to a velocity field of frequency f, i.e., if the chamber was initially excited with an 1T sound field of frequency f_{1T}, the anemometer would have as its output a signal with a strong $2f_{1T}$ component.

It was found that three types of self-sustained operation could occur in the chamber for which $2f_{1T} = f_{2T,\ 2L}$, depending on the time delay or phase change in the loop: (1) steady in waveform and level, having frequency components at f_{1T} and at its higher harmonics; (2) unsteady in waveform and level, having frequency components at f_{1T} and its higher harmonics; and (3) transitional in waveform and level having frequency components at $f_{1T,}$ $f_{1T,\ 1L}$ and higher harmonics of each. Figure 3 is a map of the lower limit of gain for self-sustenance at various values of time delay, with the type of sound field resulting indicated by the symbols. These results can be partially explained using the results of the linear-feedback experiments and calculations of the net phase change through the loop for the fundamental and second harmonic frequencies, the results of which are listed in Table 1.

Table 1. Net Phase Change Through the Loop at Various Time Delays for f_{1T} and $2f_{1T}$

Time Delay, msec	Net Phase Change, degrees	
	f_{1T}	$2f_{1T}$
22.69	359	359
22.80	39	78
23.00	111	222
23.21	183	7
23.34	232	104
23.70	360	359

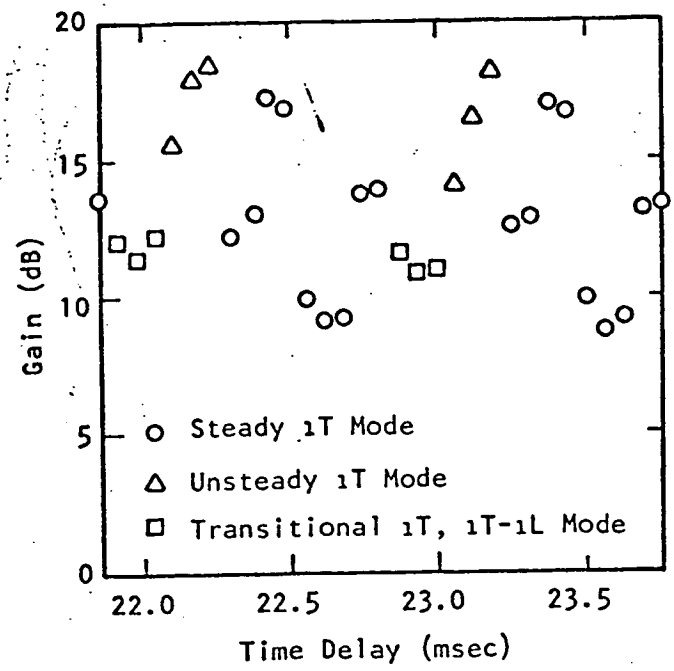

Figure 3. Self-Sustained Map of the Hot-Wire Closed-Loop System ($2f_{1T} = f_{2T,\ 1L}$ chamber)

First, Figure 3 follows a repetitive pattern. The basic pattern is that recorded between 22.69 and 23.70 msec. This span of time delay, 1.01 msec, is equal to one period of a signal at f_{1T}. Starting at 22.69 msec, the net phase changes for the f_{1T} and $2f_{1T}$ components are both 359 degrees. Since the existing and feedback sound fields are almost in phase, a minimum amount of gain is needed in the loop. At 22.80 msec, where the net phase changes are 39 and 78 degrees respectively, more gain is needed for self-sustenance. At 23.21 msec, the net phase changes are 183 and 7, respectively. Since the fundamental feedback component is almost 280 degrees out of phase with the existing fundamental component, the gain required becomes a maximum. When the existing and feedback sound fields are 180 degrees out of phase, the level of the feedback sound field must be greater than that of the existing field if self-sustenance is to be attained--the sound fields at f_{1T} are constantly interfering with each other. The

level of the self-sustained sound field is unsteady but the frequency components remain the same. This behavior resulted in the closed-loop sound field appearing "unsteady." At a time delay of 23.34 msec--another relative minimum region--the net phase change for the f_{1T} and $2f_{1T}$ components are 232 and 104 degrees, respectively. Both values of time delay are significantly different than 180 degrees so less gain is needed for self-sustenance, but not as little gain as at 23.70 msec where the phase changes have returned to 360 and 359 degrees, respectively.

One time delay in Table 1 has not been mentioned--23.00 msec, at which the net phase changes are 111 and 222 degrees, respectively. These values of net phase change differ from zero by more than they do at 22.80 msec and, hence, should require more gain instead of less for self-sustenance. However, another factor effects the results at 22.80 msec. As mentioned earlier, a 1T, 1L sound field and its higher harmonics sound fields existed along with the 1T sound field and its higher harmonic sound fields in this transitional region. This second series of sound fields reduces the gain needed for self-sustenance. This new sound field appeared in some cases due to the following characteristics: (1) $f_{1T,\ 1L}$ was 1135 Hz while f_{3T} was 2262 Hz. Hence, f_{3T} was approximately twice $f_{1T,\ 1L}$. This is similar to $2f_{1T} = f_{2T,\ 2L}$. It was concluded that whenever a resonant frequency was twice another resonant frequency, a self-sustained closed-loop sound field would be possible if the gain was high enough and the time delay was close enough to an optimal value. For this reason, the appearance of $f_{1T,\ 1L}$ and its higher harmonics, at certain time delays, was to be expected. (2) The 1T, 1L sound field requires more energy to drive (it is less responsive) than a 1T sound field. Also, f_{3T} is not exactly twice $f_{1T,\ 1L}$. Hence, for most time delays, the self-sustained sound field is naturally dominated by f_{1T} and its harmonic harmonics and $f_{1T,\ 1L}$ does not develop.

Another significant finding of the nonlinear experiments was that the resultant closed-loop sound fields do not depend on the form (frequencies and phases) of the exciting sound field. However, the gain required to initiate self-sustenance did vary with the waveform and level of the exciting sound field. When the open-loop sound-pressure levels for various resonant modes were the same, the minimum gain required to initiate self-sustenance occurred when the exciting sound field was the 1T field. Also, for a given exciting sound field, the higher the sound-pressure level, the lower the gain required to initiate self-sustenance.

Other closed-loop nonlinear feedback experiments were also carried out with the chamber for which $2f_{1T} = f_{2T,\ 2L}$. They confirmed the results discussed here.

Finally, of great significance, it was not possible to achieve self-sustenance in the chamber for which $2f_{1T}$ was not a resonant frequency.

C. Theoretical Analysis of the Anemometer Output Signal

To fully understand the nonlinear-feedback experimental results, it was necessary to analyze the anemometer output which resulted upon exposure of the hot-wire sensor to various sound fields.

Considering only the 1T mode, the bridge voltage of the anemometer was calculated. In Figure 4 the AC bridge voltage is plotted versus dimensionless time. (The curve is flat in the vicinity of $\omega t = 0, \pi$ and 2π becasue of the assumption that whenever the calculated values of E, using Equations (1), are less than E_o, the no-flow anemometer output, E, is set equal to E_o. This means that during periods of low or zero air velocity, the bridge voltage is equal to E_o.) Performing a Fourier series analysis, the harmonic components of the analytically predicted AC bridge voltage resulting from a 1T sound field can be calculated. They are shown in Figure 5. The AC signal is clearly dominated by the second harmonic,

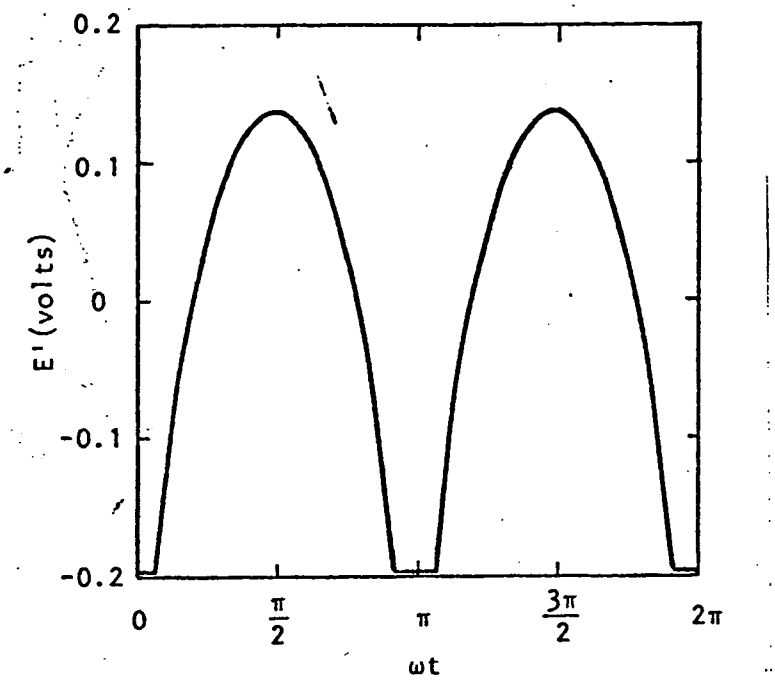

Figure 4. Analytically Predicted AC Bridge Voltage of the Anemometer Responding to a 1T Sound Field

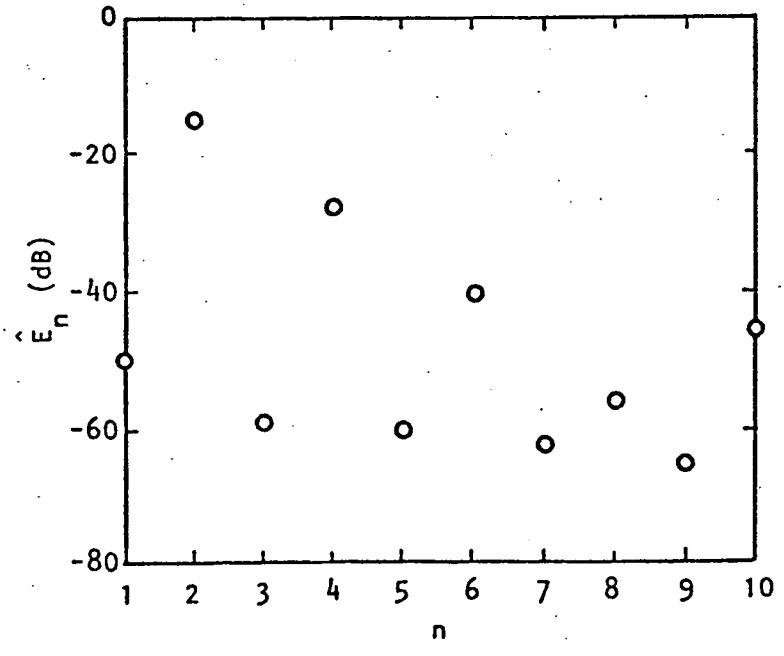

Figure 5. Harmonic Components n of the Analytically Predicted AC Bridge Voltage of the Anemometer in Response to a 1T Sound Field

which is typical of the rectification process. The presence of the first harmonic is primarily due to the temperature difference terms $[T_w - T]$ in Equations (1).

Considering a "distorted" sound field produced by the summation of a $_1T$ and a $_2T$, $_2L$ sound field, the bridge voltage for various values of P_{21} was calculated, where P_{21} is the ratio of the amplitude of the sound pressure of the $_2T$, $_2L$ sound field to that of the $_1T$ sound field and a Fourier series analysis was performed. The results are shown in Figure 6 and 7. It can be seen that distortion increases the component of E' at the fundamental frequency and that it decreases the component of E' at the second harmonic.

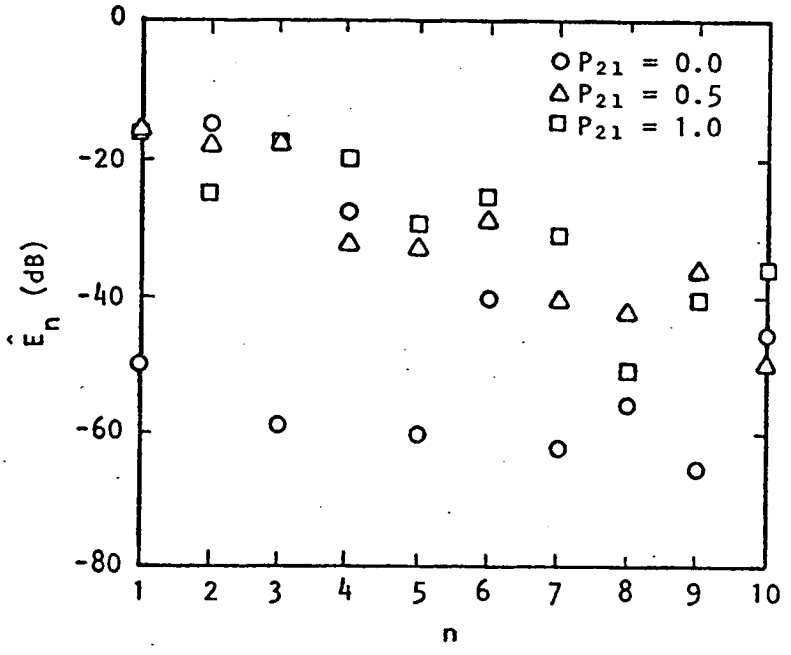

Figure 6. Harmonic Components n of the Analytically Predicted AC Bridge Voltage of the Anemometer for P_{21} = 0, 0.5, and 1.0

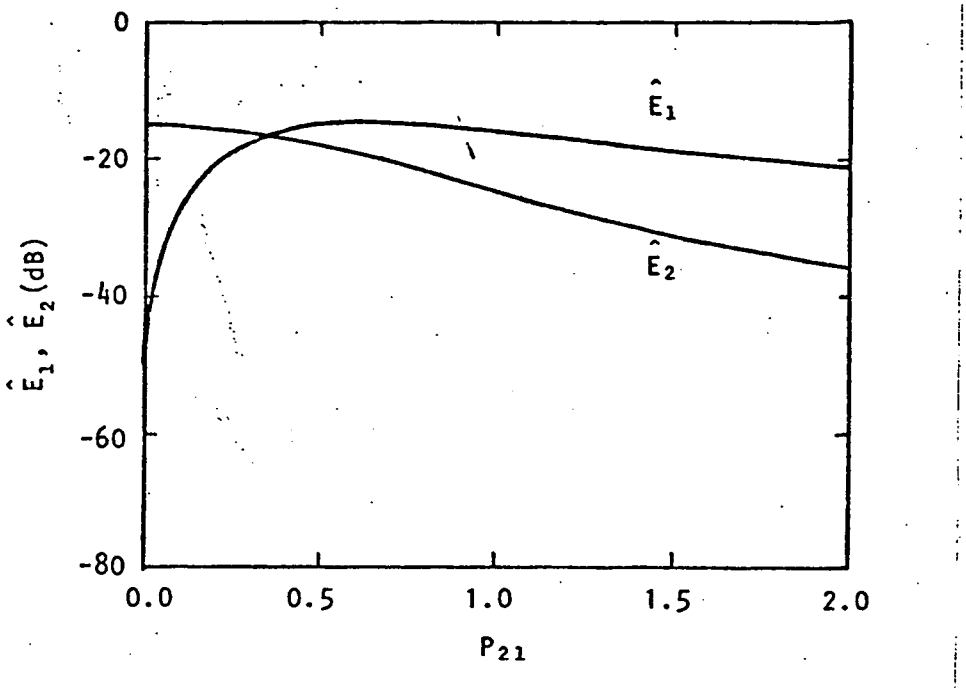

Figure 7. Variations of the First Two Harmonic Components of the AC Anemometer Voltage with P_{21}

D. Discussion of Closed-Loop Analog Investigations

From the experimental and analytical nonlinear feedback investigations discussed in the previous two sections, a general description of the transition process from an open-loop sound field to the resultant closed-loop sound field can be given phenomenalogically without describing the details for individual circumstances.

Consider that an open-loop sound field at some resonant frequency f is triggered in the chamber. An AC anemometer voltage results which has the frequency characteristics shown in Figure 5. There are components at all frequencies, f, 2f, 3f, etc., but the components at the even frequencies dominate, with the 2f component being strongest. When this signal continues around the loop and replaces the initial open-loop signal (i.e., when the loop is closed), the produced sound field (feedback sound field) is predominately at 2f--twice that of the pre-existing sound field.

The acoustics of the chamber are important here. If 2f is a resonant frequency of the chamber, a relatively strong 2f acoustic field will develop. If it is not, even if the driving at this frequency is strong, the acoustic field at 2f will be weak. Also, the higher harmonic components of the feedback signal will not result in strong acoustic disturbances at these frequencies, first, because it is unlikely that they are also resonant frequencies, and second, because even if they were resonant, it is relatively more difficult to drive the higher resonant frequencies than the lower resonant frequencies.

When the two sound fields, the initial at f and the feedback at 2f, combine, the resulting sound field contains both frequencies. The hot-wire senses this new sound field and responds with an AC anemometer voltage that has both fundamental and second harmonic components. Again, the acoustics of the chamber play an important role. The chamber selectively responds at f and 2f, when these are resonant frequencies, and does not respond well to the higher harmonic components of the input signal. The dependence of the components of the anemometer signal at f and 2f on the relative magnitude of the acoustic field in the chamber at f and 2f was shown in Figure 7. Figure 7 indicates that adding even a relatively low level acoustic field at 2f compared to the initial f acoustic field results in a significant component of the feedback signal being at the fundamental frequency f.

Again, the new feedback sound field is superimposed upon the existing sound field which also consists of the fundamental and second harmonic components, and a new feedback signal is sent to the driver. Similar existing-feedback interaction (closed-loop) processes will continue as long as the sound field exists.

The above discussion explains why an acoustic field having components at both f and 2f results from the anemometer analog system. The two-frequency

characteristic is a result of the nonlinear nature of the feedback mechanism and the acoustics of the chamber. In addition to the factors mentioned above, the amount of time delay or phase change in the loop is also of importance. The more out of phase the feedback signal is with respect to the initial perturbation in the chamber, the more amplification will be needed for self-sustenance as was illustrated by Figure 3.

Because of the nonlinear character of the hot-wire response, all the self-sustained closed-loop sound fields of the hot-wire closed-loop operation must contain higher harmonic components. If the chamber is not responsive at the 2f frequency, i.e., if 2f is not a resonant frequency (or close to a resonant frequency), the sound field will have difficulty being sustained; hence, the geometry of the chamber is or primary importance.

More extensive discussions of the experimental closed-loop investigations can be found in [8], [12], [13], [14], and [15].

Gasdynamically Induced Second Harmonic Sound Fields

The closed-loop experimental studies indicated that the second harmonic sound field played an important role in instability. The second harmonic could originate from two sources. It could be directly driven by the primary energy source (combustion in rocket engines; the acoustic driver of the analog process); or it could result from nonlinear gasdynamic effects which cause resonant acoustic fields at a given frequency to induce sound fields at higher harmonic frequencies. In the closed-loop work it was not entirely clear how much second harmonic was contributed by each source; hence, an investigation was made of gasdynamically induced second harmonic sound fields.

The object of these experiments was to determine the intensity and spatial distribution of the gasdynamically induced second harmonic sound fields. Three chamber configurations were used: one in which $2f_{1T} = f_{2T,\ 2L}$; one

in which $2f_{1T} = f_{1T,\ 3L}$ and one in which the doubled frequency was not a resonant frequency, $2f_{1T} = f_x$. Three investigations were carried out. First, each chamber configuration was driven at f_{1T} at a particular sound level and the resultant second harmonic (2s) sound field was probed ($2f_{1T} = f_{2s}$), at five different sites, to determine the variation in amplitude and phase. Then, one location was chosen, and the amplitude of the 1T sound field was varied and the level of the resulting 2s was measured. Lastly, the location of the driver was changed to determine the effect of driver location.

Initially it was expected that, for those chambers for which f_{2s} was a resonant frequency, the 2s would have the amplitude and phase characteristics of the resonant sound field. This was found to be only partially true. The results of the first experiments showed the gasdynamic (2s) sound fields were dependent on chamber geometry--changing the length of the chamber changed the spatial distribution of the second harmonic. Some effort was directed at characterizing the various 2s sound fields. The distributions appeared to be a combination of the resonant sound field closest in frequency to f_{2s}, plus an additional component. The additional component appeared to be in part composed of a radial acoustic mode and in part some unknown component. Also, the results were compared to the analytically predicted gasdynamic sound fields obtained by Maslen and Moore [16]. The comparison indicated the 2s was not entirely described by Maslen and Moore, but was closer to being a summation of the Maslen and Moore prediction, plus an additional component having the form of the resonant sound field closest in frequency to f_{2s}. The work involved in trying to obtain analytical expressions which would characterize the measured 2s sound fields was extensive when compared to the usefulness of the results obtained, so these efforts were terminated.

The results of the second experiments showed that the level of the 2s was dependent on the level of the fundamental and that to obtain a significant

amount of gasdynamically generated second harmonic, an intense fundamental sound field would be required. Typical results for the $2f_{1T} = f_{1T,\,3L}$ chamber are shown in Figure 8. This figure plots the ratio of the intensity of the 2s sound field, at a particular location in the chamber, to the intensity of the 1T sound field against the relative intensity of the 1T sound field, when compared to ambient pressure. There were only relatively small variations in the results for the other two chamber configurations.

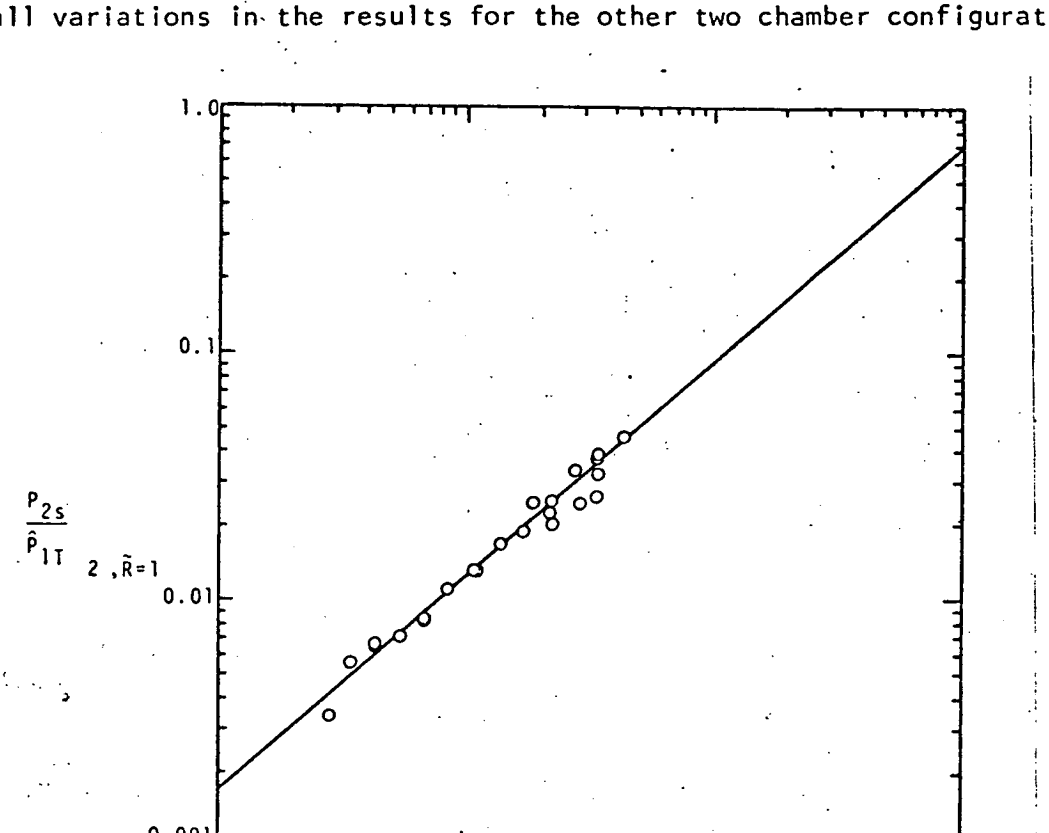

Figure 8. Relative Amplitude of the Gasdynamic Second Harmonic Sound Field as a Function of the Amplitude of the Fundamental Sound Field at Probe Site 2 at $\tilde{R} = 1.0$ [17].

When the location of the driver was changed, it was found that the overall amplitude of the second harmonic sound fields were of the same order of magnitude as had existed previously. A variation did occur in the spatial distribution of the second harmonic in some cases. The cause of this is unknown but is probably a combination of several factors. For instance, there were always slight irregularities in the driver sound field--the first tangential. These irregularities in the fundamental varied with driver location and from experiment to experiment. Since the fundamental was the origin of the gasdynamic second harmonic, some changes in the second harmonic were to be expected. Also, the driver location used initially was a good location for actually driving a second harmonic resonant sound field; the later driver location was not.

Further details of the second harmonic studies can be found in [17], [18], and [19].

The above studies of the gasdynamically induced second harmonic sound fields gave some insight into the nature of these sound fields, but did not evaluate the contribution of these sound fields to instability. A different type experiment was needed for that purpose. The twin-chambers investigations served that need.

Twin-Chambers Investigations

Simulation of actual combustion is attained in the experimental system by operating in the closed-loop mode--the sensor responds to oscillations in the chamber and an electrical output results, which is amplified, phase-shifted and/or time delayed, and the resulting signal sent to an acoustic driver mounted on the chamber, which in turn generates new oscillations, and so on. Altering the various parameters in the loop, such as amplification or phase, alters the operating characteristics; for example, the oscillations may die out or become very intense. This usually occurs

so rapidly that it becomes difficult to make detailed studies of the phenomena and their relationships to one another. To overcome these difficulties, use of a twin-chambers system was initiated.

Referring to Figures 9 and 10, for the twin-chambers studies, the driver on the first chamber, chamber A, was activated by a signal originating from some combination of signals from two function generators. This resulted in oscillations in chamber A, to which the sensor responded. The resulting signal was then amplified and sent to the driver on the second (or twin) chamber, chamber B, which resulted in oscillations in B. This would have been the feedback sound field in A if chamber A were operating closed-loop. The signals to the drivers and/or the sound fields in each chamber were then compared and these comparisons indicated whether or not a single chamber operating closed-loop under the same conditions would be stable or unstable. (If the fundamental and second harmonic

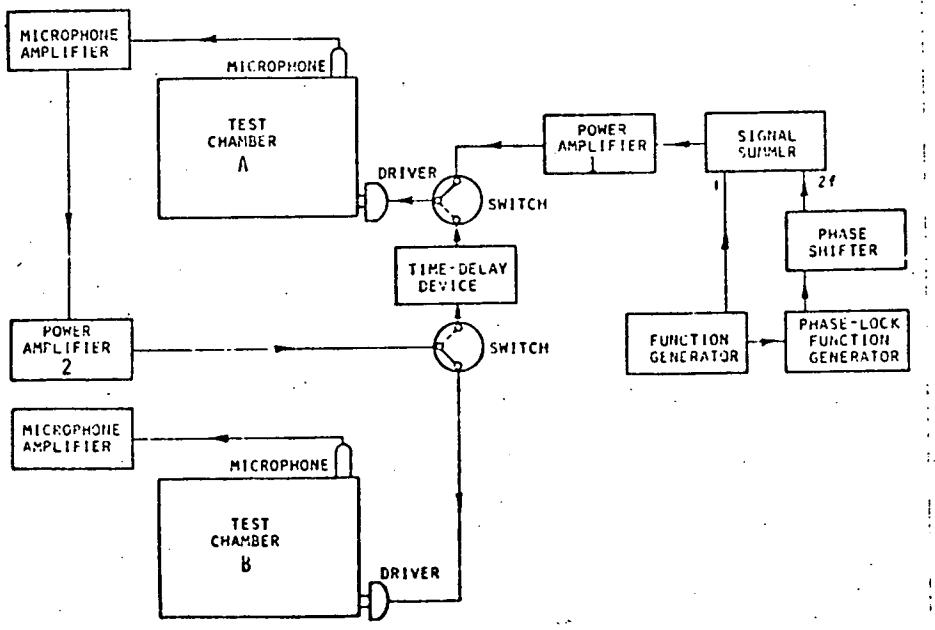

Figure 9. Schematic Diagram of the System Used for Pressure Sensitive Open-Loop Simulation of Closed-Loop Operation [17].

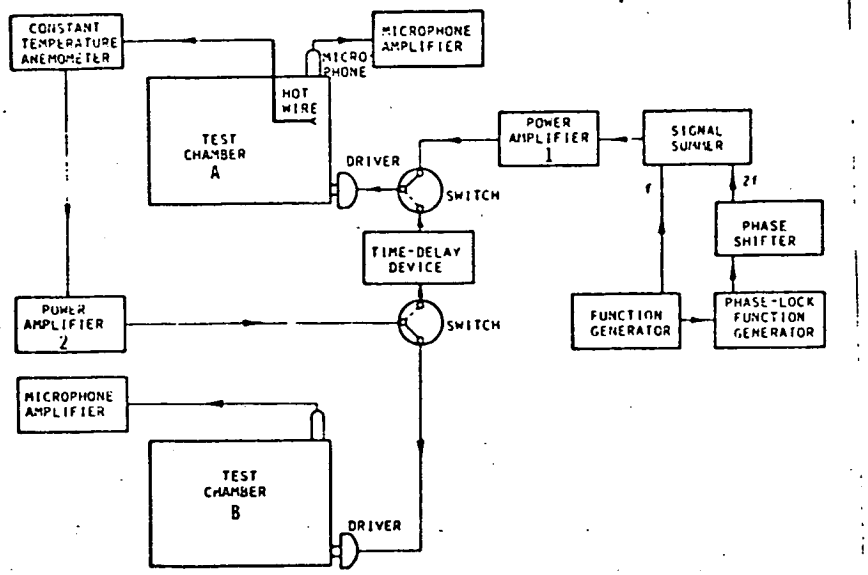

Figure 10. Schematic Diagram of the System Used for Velocity Sensitive Open-Loop Simulation of Closed-Loop Operation [17].

frequency components of the feedback sound field were in phase with, and had the same or greater amplitudes than the original sound field, oscillations would be sustained or magnified if the system were operated closed-loop.)

The object of the studies was to examine the effect of second harmonic content on the operating characteristics of the two types of systems--the one having a linear feedback mechanism (a microphone which responds linearly to pressure fluctuations) and the one having a nonlinear feedback mechanism (the constant-temperature hot-wire anemometer which responds nonlinearly to velocity fluctuations)--, to examine the importance of second harmonic to self-sustained closed-loop operation and to determine the intensity of the second harmonic for those situations for which self-sustenance was predicted. Three sets of twin-chambers were used--the $2f_{1T} = f_{2T,\ 2L}$, the $2f_{1T} = f_{1T,\ 3L}$, and the $2f_{1T} = f_x$.

For the linear system, referring to Figure 9, the procedure was as follows. Initially the two function generators were set to produce signals at $f = f_{1T}$ and 2f. These signals were summed and sent to the driver on chamber A. The microphone sensed the resulting sound field and the output of the microphone was amplified and sent to the driver on chamber B. The phase between the initial signals at f and 2f were adjusted until the phase between the f and 2f components of the sound field in A was the same as the phase between f and 2f in B. Next, the amplifiers were adjusted so that the amplitude of the pressure at f in A and B was the same. The amplitude of the signal at 2f to the summer was then varied between zero and the upper limit of operation of the system and the levels of the resulting sound fields in each chamber was noted. (After this adjustment there was still a relative time delay between the sound fields in the two chambers--the time delay necessary in the loop for sustained closed loop operation.)

Figures 11 and 12 are typical of the results obtained for the linear system. The following observations can be made. Referring to Figure 11, with no second harmonic voltage to the driver of chamber A, primarily gasdynamic second harmonic content existed in each chamber. As second harmonic voltage was added to chamber A, a lesser amount of second harmonic resulted in chamber B. The amount of second harmonic in chamber B was always less than that in A. Adding second harmonic to A did not alter the amplitude of be fundamental sound field in B. The only conditions under which the sound fields in each chamber matched occurred when A was not being driven at the second harmonic frequency--when primarily gasdynamic second harmonic existed. Figure 12 shows the amount of second harmonic content under these conditions for the three chamber sizes.

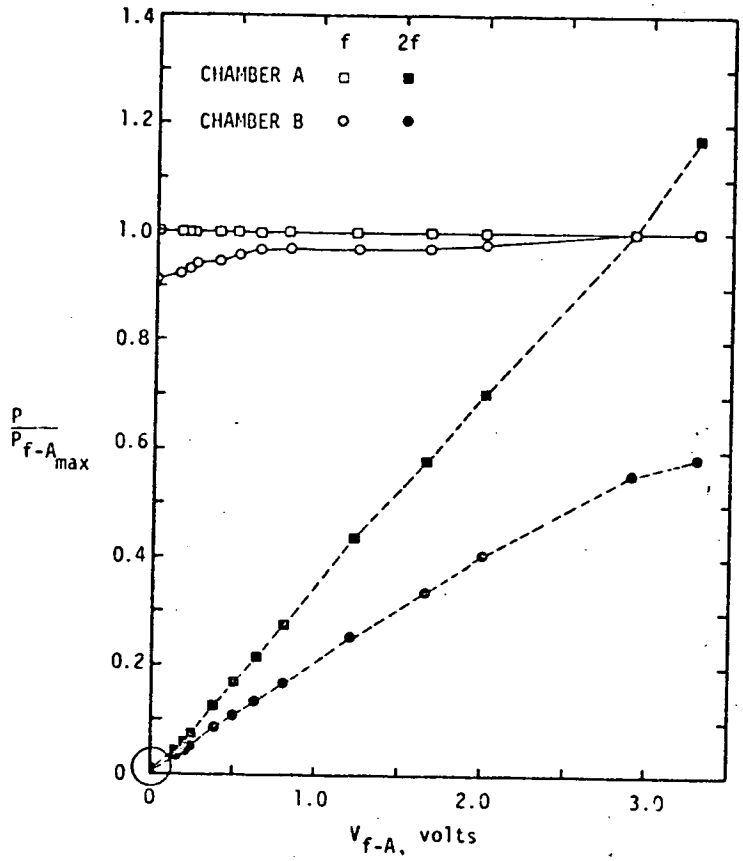

Figure 11. Levels of the Sound Fields at f and 2f in Chambers A and B as a Function of the Voltage at 2f to the Acoustic Driver on Chamber A; Linear System; $2f_{1T} = f_{1T,\ 3L}$ [17].

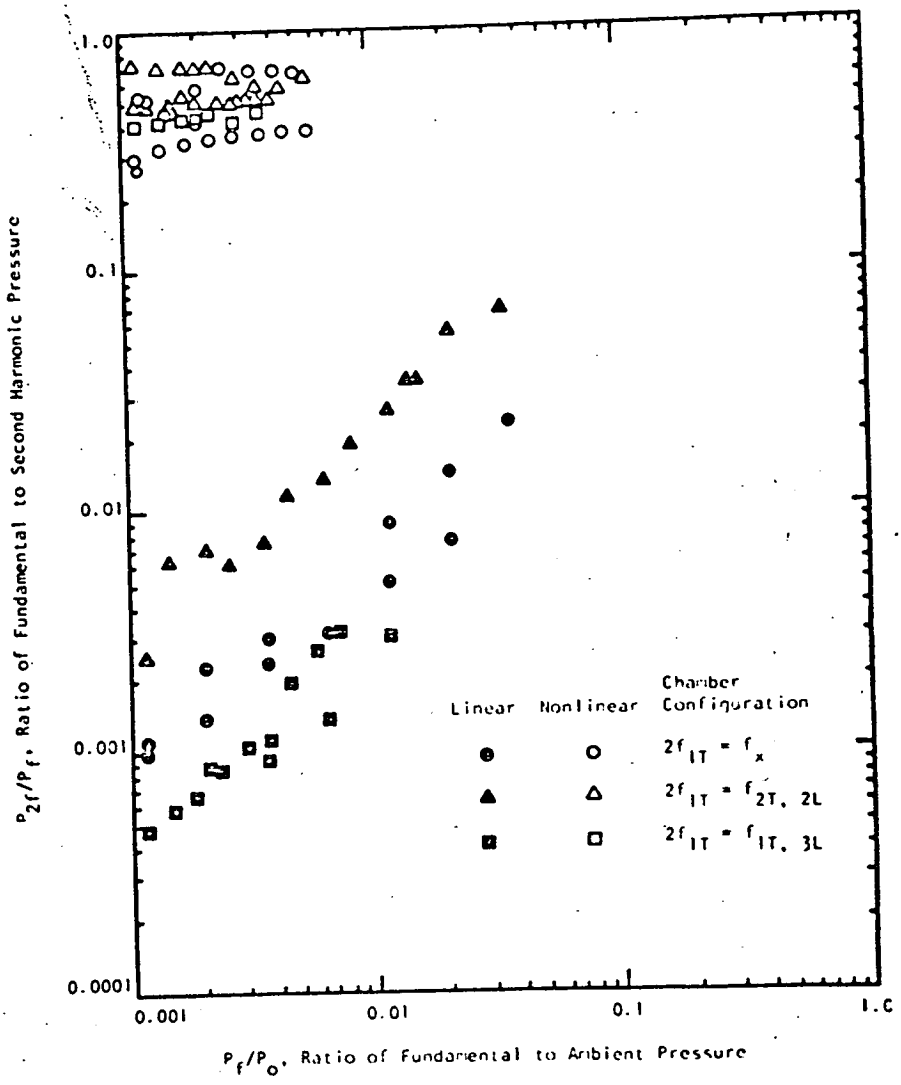

Figure 12. Relationship Between Fundamental and Second Harmonic Sound Fields as a Function of Intensity of Fundamental [18].

With a linear system, there was no natural mechanism which would enable any significant second harmonic oscillation other than the gas-dynamic one to be sustained during closed-loop operation. If a perturbation occurred in the chamber at the second harmonic frequency, this perturbation would tend to die out. The second harmonic content would not be necessary for self-sustained closed-loop operation. These general results did not strongly depend on chamber geometry; similar results were obtained for all three chamber lengths. The results are consistent with the results of the closed-loop experiments.

For the nonlinear system, referring to Figure 10, the procedure was as follows. Initially, the two function generators were set to produce signals at $f = f_{1T}$ and 2f. These signals were summed and sent to the driver on chamber A. The hot-wire sensed the sound field generated and the resulting output of the anemometer was amplified and sent to the driver on character B. The phase between the initial signals at f and 2f was adjusted until the phase between f and 2f of the sound field in A was the same as the phase between f and 2f in B. Next, the amplifiers were adjusted so that the amplitudes of the pressure at f and 2f in A matched the amplitudes of the pressure at f and 2f in B, respectively. The amplitude of the signal at 2f to the summer was then varied from zero to the upper limit of operation of the system and the variation in the results sound fields recorded. (Again, a time-delay existed between the sound fields.)

Figures 12 and 13 are typcial of the results obtained for the nonlinear system. The following results were observed. With no second harmonic voltage to the driver of chamber A, the sound field in B was dominated by second harmonic content. As second harmonic voltage was added to A, the amount of second harmonic content in the sound field in B decreased in the chambers for which $2f_{1T} = f_{1T,\ 3L}$ at $2f_{1T} = f_{2T,\ 2L}$ and remained approximately the

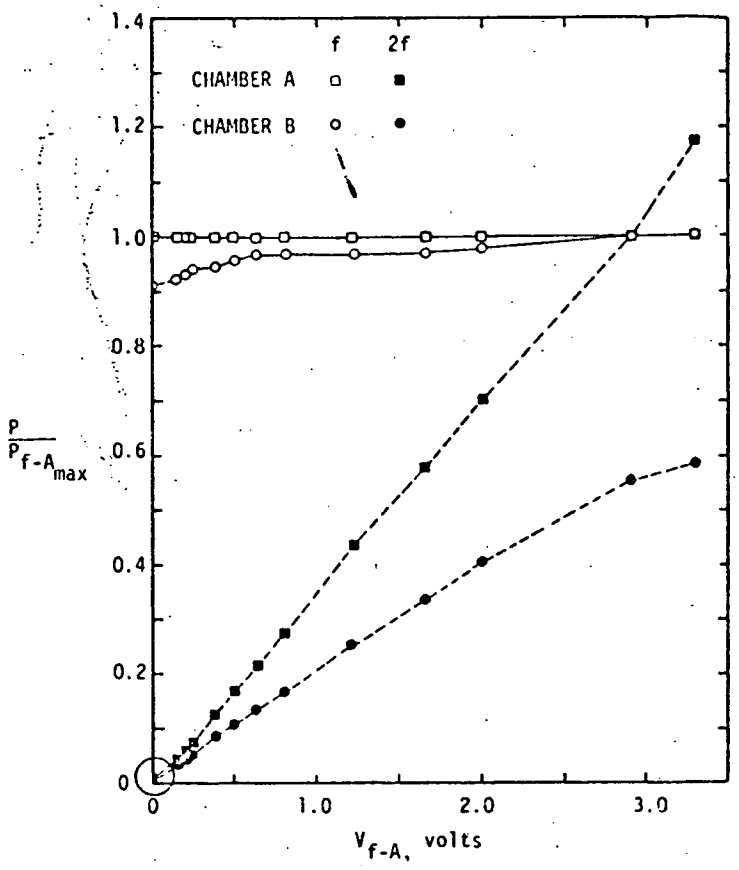

Figure 13. Levels of the Sound Fields at f and 2f in Chambers A and B as a Function of the Voltage at 2f to the Acoustic Driver on Chamber A; Nonlinear System; $2f_{1T} = f_{1T,\ 3L}$ [17].

same in the chamber for which $2f_{1T}$ = fx. There was an amount of second harmonic voltage which, when added to A, resulted in the same amplitude for the second harmonic sound fields in both chambers. Adding second harmonic content to A increases the amplitude of the fundamental sound field in B. It was necessary to have a strong second harmonic input to chamber A in order to obtain a strong fundamental sound field in B. There was a condition under which the sound fields in each chamber had the same amplitudes at both the fundamental and second harmonic frequencies and the same phases between fundamental and second harmonic. The amount of second harmonic existing at this state is shown in Figure 12 for each of the chambers. The results for the $2f_{1T}$ = fx chamber tended to be somewhat erratic.

With the nonlinear system, a sound field at the fundamental frequency naturally resulted in a response primarily at the harmonic frequency. The system would not be able to sustain itself under these conditions. It would be necessary to have a driver input at both the fundamental and second harmonic frequencies in order for the sound fields in chambers A and B to match. Second harmonic content would be necessary for self-sustained closed-loop operation. This was consistent with the results of the closed-loop investigations.

What was not entirely consistent with the closed-loop results was the prediction that the chamber for which $2f_{1T}$ was not a resonant frequency could be self-sustaining. With the twin-chambers experiments it is predicted that a $2f_{1T}$ = fx chamber could be self-sustaining if enough feedback amplification were available in the loop. (A factor which is not noted in the figures is that it took approximately twice as much power to achieve the "matched" situation for the $2f_{1T}$ = fx chamber as it did for either the $2f_{1T} = f_{1T,\ 3T}$ or $2f_{1T} = f_{2T,\ 2L}$ chambers.) The twin-chambers results indicate that, if the closed-loop experiments had had a more powerful amplifier and an acoustic driver able to withstand higher power input, perhaps closed-loop, self-sustained operation would have been achievable.

Further discussion of the twin-chambers investigations can be found in [17] and [18].

Mathematical Modeling.

This research was begun because of a desire to determine whether or not certain effects that had been observed experimentally could be predicted mathematically. It was felt that this would be helpful in explaining the experimental results to other engineers and scientists and in interpretation of the observed phenomena. In order that the predictions of the analytical work could be easily understood, it was desired to avoid methods which required the simultaneous numerical solution of a system of partial differential equations. For this reason, the method of Powell [10], who analyzed pressure-sensitive combustion instability problems, was attractive. Powell [10] used certain approximations to deduce a single nonlinear wave equation governing a velocity potential and then solved this equation approximately using the Galerkin method. It was decided to use a similar methodology for the analysis of velocity-sensitive combustion instability problems.

It was found that if a set of approximations slightly different from those used in [10] was employed, a wave equation could be derived which contained gasdynamic nonlinearities of all orders, rather than only those of order two as in [10]. The assumptions involved in this analysis are discussed by Peddieson, Ventrice, and Purdy [18] and further details are given by Wong [20]. The appropriate wave equation is (in dimensionless form)

$$\partial_{tt}\Phi + \vec{\nabla}\Phi \cdot \vec{\nabla}\left(2\partial_t\Phi + \vec{\nabla}\Phi \cdot \vec{\nabla}\Phi/2\right) - \nabla^2\Phi\left[1 - (\gamma - 1)\cdot\right. \tag{4}$$

$$\left.(\partial_t\Phi + \vec{\nabla}\Phi \cdot \vec{\nabla}\Phi/2)\right] + W\left[1 - (\gamma - 1)\partial_t\Phi + \vec{\nabla}\Phi \cdot \vec{\nabla}\Phi/2)\right]^{(\gamma-2)/(\gamma-1)} = 0$$

where $\vec{\nabla}$ is the gradient operator, Φ is the velocity potential, W is the burning rate, γ is the ratio of specific heats for a perfect gas and t is time.

To be consistent with the work of previous investigators, and to simplify the computation effort, it was decided to develop a second-order form of (4). This was done by assuming that

$$\Phi = \varepsilon[\bar{\phi}(z) + \phi(x, y, z; t)]$$
$$W = \bar{w}(z) + \varepsilon w(x, y, z, t) \tag{5}$$

where ε is a measure of the initial disturbances, z is the axial coordinate (parallel to the main flow) in the combustor, and the quantities with the superposed bar are associated with the mean flow. Substituting (5) into (4), assuming $\bar{w} = 0(\varepsilon)$ and $w = 0(\varepsilon)$, neglecting all terms of $0(\varepsilon^3)$ and dividing by ε, one obtains

$$\partial_{tt}\phi + \bar{w}\partial_t\phi + 2\bar{u}\partial_{zt}\phi - \nabla^2\phi + \varepsilon(2\vec{\nabla}\phi \cdot \vec{\nabla}\partial_t\phi +$$
$$(\gamma - 1)\nabla^2\phi\partial_t\phi + w) = 0 \tag{6}$$

where

$$\bar{u}(z) = \int_0^z \bar{w}d\xi \tag{7}$$

is the steady-state gas velocity. The perturbations of velocity, density, pressure, and temperature associated with ϕ are respectively

$$\vec{u} = \vec{\nabla}\phi$$
$$\rho = -[\partial_t\phi + \bar{u}\partial_z\phi + \varepsilon(u^2 - (2 - \gamma)(\partial_t\phi)^2)/2]$$
$$p = -\gamma[\partial_t\phi + \bar{u}\partial_t\phi + \varepsilon(u^2 - (\partial_t\phi)^2)/2] \tag{8}$$
$$T = -(\gamma - 1)(\partial_t\phi + \bar{u}\partial_z\phi + \varepsilon u^2/2)$$

It was first attempted to use the vaporization-limited combustion model of Priem [1] in conjunction with (6). In the present notation this can be written as

$$w = (\bar{w}/\varepsilon^2)[(1 - \partial_t\phi/2)((1 - \partial_z\phi/\bar{u}_L)^2 +$$
$$(u^2 - (\partial_z\phi)^2)/\bar{u}_L^2)^{\frac{1}{4}} - 1] \tag{9}$$

where $\bar{u}_L$ is the velocity of the liquid drops. When (9) is combined with (6), the result is a single equation for ϕ. Because of the non-polynomial nonlinearities in (9), this equation cannot be analyzed conveniently by the Galerkin method. For this reason, another version of the method of weighted residuals, the orthogonal collocation method, was used. The details of this method are discussed in [18] and [20]. It was eventually concluded that this method was unreliable when applied to this type of problem and was abandoned. It is believed that this unreliability is related to the fact that the nonlinear terms in (6) have the correct form only for moderate values of ε. This can be illustrated by the following example.

Consider a nonlinear elastic system governed by the equation

$$\ddot{f} + f + \varepsilon N\ (f, \dot{f}) = 0 \tag{10}$$

where f is the displacement, N is a nonlinear function, $\varepsilon << 1$, and a superposed dot indicates differentiation with respect to time. Suppose

$$N(f, \dot{f}) = N_o\ f\dot{f} + 0(\varepsilon) \tag{11}$$

Then the second order form of (10) would be

$$\ddot{f} + f + \varepsilon N_o\ f\dot{f} = 0 \tag{12}$$

This equation can be integrated once to yield

$$\log[(1 + \varepsilon N_o \dot{f})/(1 + \varepsilon N_o \dot{f}_o)] - \varepsilon N_o(\dot{f} - \dot{f}_o) - \varepsilon^2 N_o^2\ (f^2 - f_o^2)/2 = 0 \tag{13}$$

where

$$f(0) = f_o,\ \dot{f}(0) = \dot{f}_o \tag{14}$$

For $\varepsilon N_o << 1$, (13) can be simplified to

$$f^2 + \dot{f}^2 - 2\varepsilon N_o \dot{f}^3/3 + 0(\varepsilon^2 N_o^2) = f_o^2 + \dot{f}_o^2 \tag{15}$$

This is consistent with the original approximation leading to (12). For $\varepsilon N_o << 1$ it is expected that the solution of (12) will be a resonable approximation to the solution of (10). Equation (15) indicates that the solutions are periodic as one would expect for free vibrations of an elastic system.

Suppose that N_o is sufficiently large so that the inequality $\varepsilon N_o << 1$ is not satisfied. Then (12) is not a rational approximation to (10) and the solution of (12) may not have the characteristics of an elastic system. As an example, consider $\varepsilon N_o >> 1$. Then (13) can be simplified to

$$\dot{f} = \dot{f}_o \exp\left[\varepsilon^2 N_o^2 (f^2 - f_o^2)/2\right] \tag{16}$$

For $f_o = 0$ this becomes

$$\dot{f} = \dot{f}_o \exp(\varepsilon^2 N_o^2 f^2/2) \tag{17}$$

In this case the solution is not periodic and grows without bound. The application of the collocation method to (6) produces a set of nonlinear ordinary differential equations governing the values of ϕ at the collocation points. These equations contain nonlinear terms similar to the last term in (12). It appears that most choices of collocation points cause the coefficients of some of these terms (equivalent to εN_o) to become sufficiently large so that the equations predict behavior similar to that indicated by (17). This happens even in the absence of combustion terms. It may be that more success could be achieved by applying the collocation method directly to (4), but this matter was not pursued.

Since the collocation method could not be made to produce satisfactory results, it was decided to employ the Galerkin method. As mentioned previously, this method cannot be used in conjunction with (9). Thus, (9) was replaced for purely velocity sensitive combustion with

$$w = \bar{w}\, n\, u^2 \tag{18}$$

where n is called the interaction index. This is analogous to the customary treatment of pressure sensitivity (see, for instance, Powell [10]). As in the case of pressure sensitivity, (18) can be generalized to account for history effects as

$$w = \bar{w}\, n\, (u^2 - u_\tau^2) \tag{19}$$

where $u_\tau(x, y, z, t) = u(x, y, z, t - \tau)$ and τ is called the time lag. Equation (18) can be related to burning-rate laws meant to apply to special types of combustion processes such as (9). For an example of this, see Wong [20, 21]. With the use of (19), it was possible to achieve significant progress.

Peddieson, Wong, and Ventrice [19] discussed the application of (6) and (19) to transverse wave motion in a cylindrical combustion chamber. An approximate solution, based on the 1T, 1R, and 2T acoustic modes of the chamber, was used and the Galerkin method was employed to carry out a modal analysis. This resulted in a system of ordinary differential equations that could be solved to determine the temporal behavior of the modal amplitudes. This was done numerically using a fourth-order Runga-Kutta method. (For further details, see [19] and [20, 21].) Stability boundaries were determined and the behavior of the pressure at the chamber wall was determined. Some typical stability boundaries are shown in Figures 14-17. It can be seen that all boundaries resemble rectangular hyperbolas in the n-ε plane. A purely velocity-sensitive system will always be stable to infinitesimal disturbances. Thus, the instabilities associated with Figures 14-17 are triggered instabilities.

It was felt that the numerical solutions discussed above could be usefully supplemented by using the method of multiple scales (see, for instance,

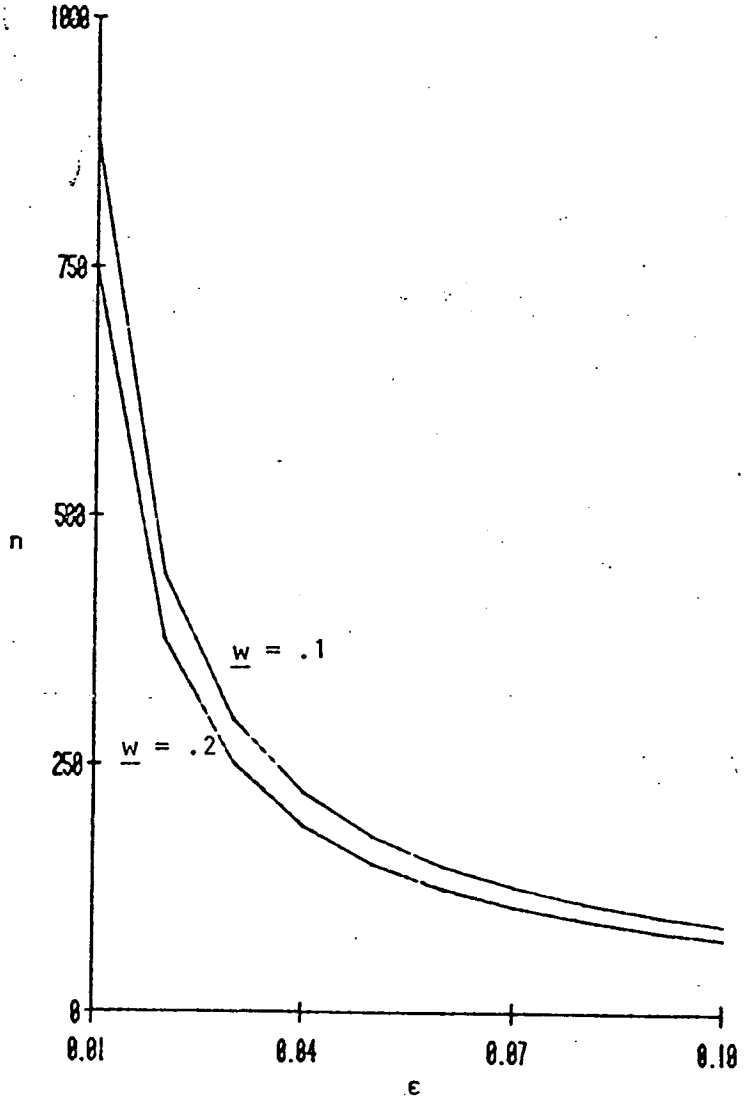

Figure 14. Stability Boundary for Standing Waves

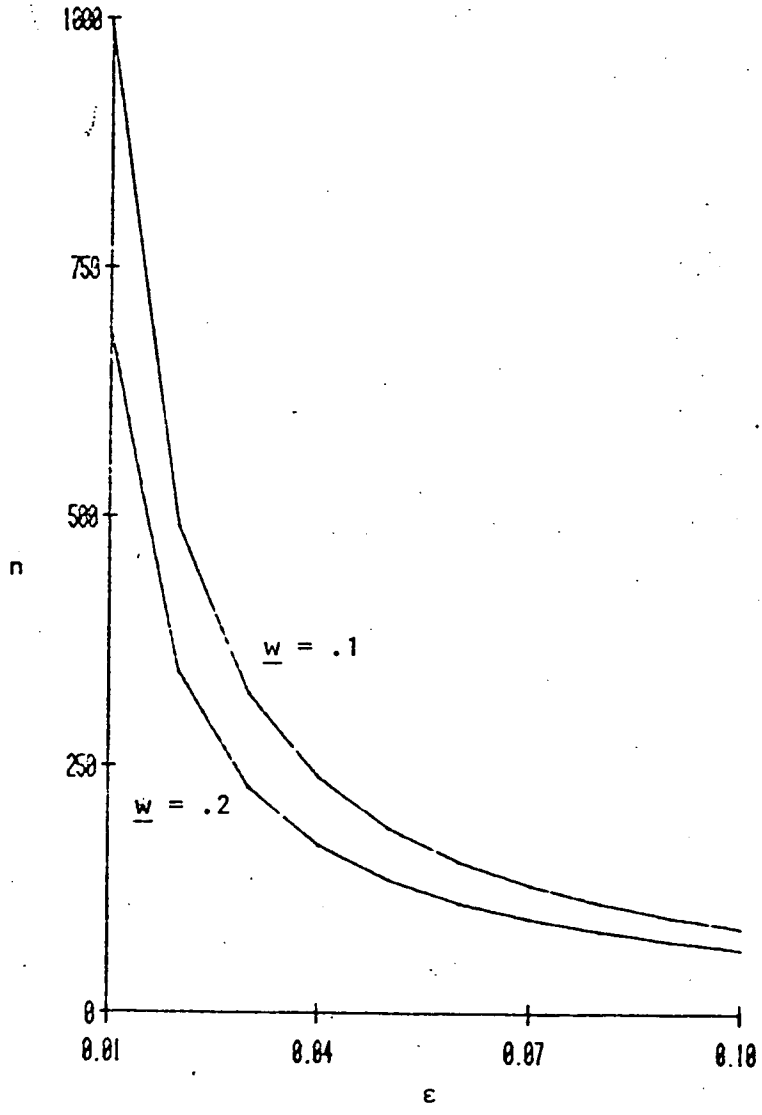

Figure 15. Stability Boundary for Traveling Waves

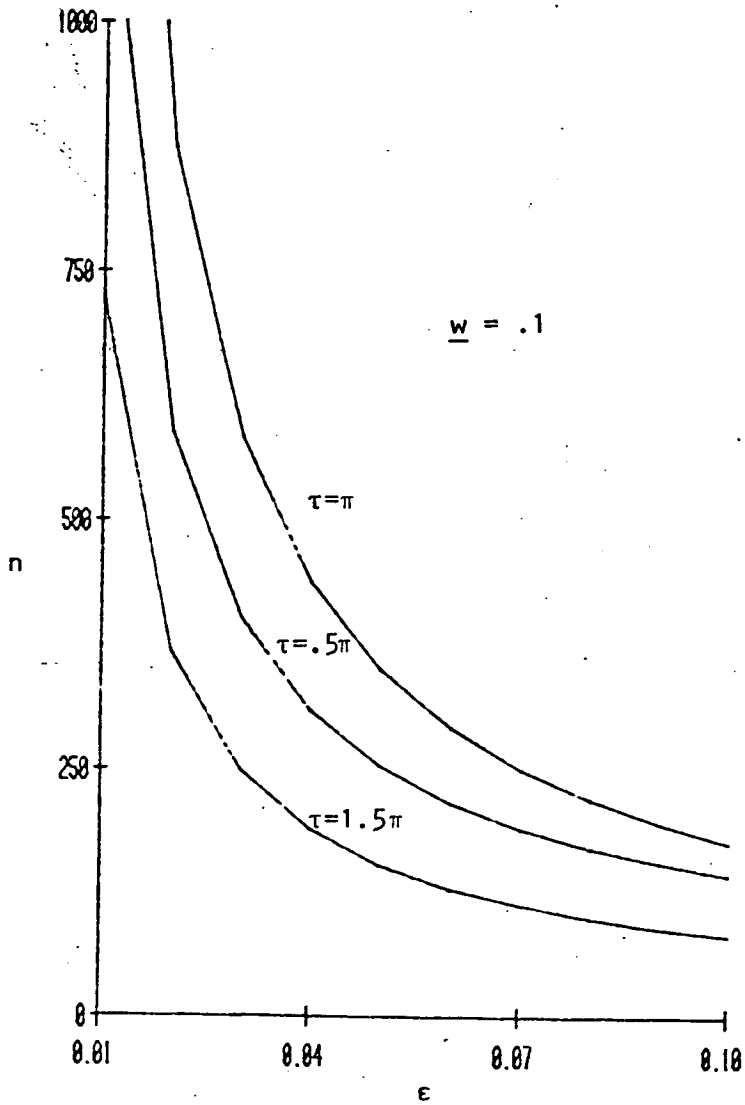

Figure 16. Stability Boundary for Standing Waves

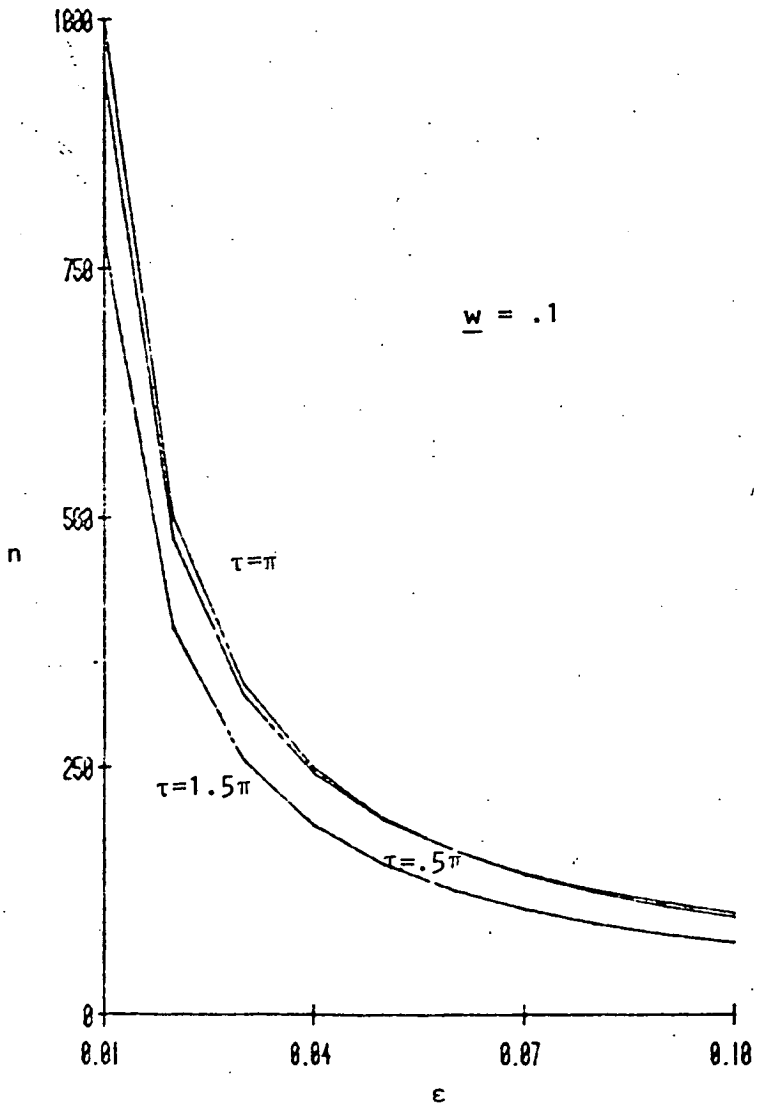

Figure 17. Stability Boundary for Traveling Waves

Nayfeh [22]) to obtain approximate analytical solutions to the governing equations for the modal amplitudes. To investigate the feasibility of doing this, Googerdy [23, 24] considered purely pressure-sensitive combustion and replaced (19) by

$$w = - \bar{w}n(\partial_t \phi - \partial_t \phi_\tau)/\varepsilon \tag{20}$$

Rather than deal with a cylindrical chamber, he considered the mathematically simpler problems of transverse motion in a narrow rectangular chamber and transverse motion in an annular chamber with a narrow gap width. The first problem is analogous to that of radial oscillations in a cylinder, while the second is analogous to the problem of combined radial and transverse motion in a cylinder. Both of these cases were treated numerically by Powell [10]. Using the method of multiple scales it was possible to produce most of Powell's results in closed form and to provide physical explanations for them. This gave confidence to the use of the perturbation method.

McDonald [25, 26] then applied the method of multiple scales to the problem of purely velocity-sensitive combustion instability in an annulus of narrow gap width. Transverse motions were treated. For standing waves, the simplest solution able to show the effect of quadratic nonlinearities has the form

$$\phi(\theta, t) = f_1(t) \cos\theta + f_2(t) \cos 2\theta \tag{21}$$

where θ is a polar coordinate which loactes radial cross sections in the annulus. Substituting (21) and r=1 into (6) and (19), using the Galerkin method to carry out the modal analysis, and assuming that the gasdynamic nonlinearities are negligible compared to the combustion nonlinearities, results in the equations

$$\begin{aligned} \ddot{f}_1 + f_1 + \varepsilon_1(\bar{\sigma}\dot{f}_1 + 2\bar{w}n\, f_1\, f_2) &= 0 \\ \ddot{f}_2 + 4f_2 + \varepsilon(\bar{\sigma}\dot{f}_2 - \bar{w}n\, f_1^2/2) &= 0 \end{aligned} \tag{22}$$

where $\bar{\sigma} = \bar{w}/\varepsilon$. Solving these equations by the method of multiple scales, subject to the initial conditions

$$f_1(0) = f_2(0) = 0, \ \dot{f}_1(0) = 1, \ \dot{f}_2(0) = 0 \tag{23}$$

leads to the uniformly-valid first approximations

$$\begin{aligned} f_1 &= \exp(-\bar{w}\,t/2)\,\sec[\varepsilon n(1-\exp(-\bar{w}\,t/2))/2^{3/2}]\,\sin t + 0(\varepsilon) \\ f_2 &= -(1/2^{3/2})\exp(-\bar{w}\,t/2)\tan[\varepsilon n(1-\exp(-\bar{w}t/2))/2^{3/2}]\cdot \\ &\quad \sin 2t + 0(\varepsilon) \end{aligned} \tag{24}$$

These simple solutions illustrate the basic features of the system. Both the secant and the tangent become infinite when their arguments take on the value $\pi/2$. Thus, if $\varepsilon n < \pi 2^{1/2}$, the arguments of the secant and tangent in (24) are less than $\pi/2$ for all t, and f_1 and f_2 approach zero as t approaches infinity. If $\varepsilon n > \pi 2^{1/2}$, on the other hand, these arguments reach $\pi/2$ in a finite time, causing f_1 and f_2 to become infinite in a finite time. The former situation is stable, while the latter is unstable. The equation of the stability boundary in the n-ε plane is

$$n = 2^{1/2}\,\pi/\varepsilon \tag{25}$$

For this situation it can be shown that

$$\begin{aligned} \lim_{t\to\infty} f_1 &= (2/\pi)\sin t \\ \lim_{t\to\infty} f_2 &= -(1/2^{1/2}\,\pi)\sin 2t \end{aligned} \tag{26}$$

Thus, a neutral oscillation is approached when mass addition due to unsteady combustion is exactly balanced by mass loss due to steady-state flow. McDonald [25, 26] has found similar solutions for traveling waves and show that the conclusions discussed above are qualitatively unchanged by the inclusion of gasdynamic nonlinearities. He has further shown that the qualitative aspects of the perturbation solutions are in agreement with those of direct numerical calculations based on (22). This work illustrates

vividly the usefulness of the combustion law (18). Closed-form solutions similar to (24) could never be obtained using a combustion law of the form (9).

Conclusions

The research has resulted in useful experimental analog and analytical techniques for the study of Reynolds number dependent processes. The techniques are general and could be applied to any Reynolds number dependent process. During the course of the research, application to combustion instability in liquid propellant rocket engines was emphasized.

Experimentally, the initial object of the work was to study the usefulness of a constant-temperature hot-wire anemometer as an analog tool for the investigation of combustion instability. To accomplish this, analytical and experimental open-loop studies of the anemometer were carried out and compared to analytical open-loop studies by Heidmann [2, 3] of vaporization limited combustion. (Open-loop studies compare existing pressure perturbations and the resulting perturbations in the burning rate in the case of combustion, or in the anemometer output in the case of the analog, in order to predict actual closed-loop operation.) The comparisons indicated qualitative agreement among the three studies--the second harmonic frequency distortial of the fundamental frequency perturbation was the important factor in the development of instability.

In closed-loop studies, the burning rate in combustion, or anemometer output in the analog process, feeds back upon itself, resulting in new pressure perturbations, which combine with the previous perturbations to form a new acoustic field, and so on. The analog was refined to run closed-loop using either the original nonlinear analog device--the anemometer--or a linear analog device--a microphone. Experiments were then run to investigate the validity of the open-loop predictions of closed-loop behavior. These studies confirmed the importance of second harmonic content to instability in the nonlinear case and gave insight into the reasons for this

importance--second harmonic content is a natural result of the nonlinearity of the process and is necessary to sustaining perturbations at both the fundamental and second harmonic frequencies.

Two important similarities in the characteristics of combustion instability and the closed-loop analog process were identified. First, in combustion instability, a minimum perturbation amplitude is necessary to excite instability. In the analog this was also true. Second, in combustion instability, an initial sinusoidal perturbation becomes harmonically distorted once instability develops. Again, in the analog this was also found to be true. These studies also indicated that chamber resonance might play a more significant role in causing instability than had been anticipated. Second harmonic content was not found to be important in the linear feedback process.

The closed-loop analog studies did not fully indicate the difference in character between linear (pressure sensitive) and nonlinear (velocity or Reynolds number sensitive) processes, so a twin-chambers technique was developed for this purpose. In the twin-chambers work, instead of having the analog device feeding back on itself, the feedback signal was sent to an identical twin chamber so that the originating and feedback perturbations could be studied separately. These studies indicated, even more clearly than the closed-loop studies, that second harmonic was an integral part of a nonlinear process and necessary to the sustenance of the fundamental frequency perturbations. They also indicated that this was not true for the linear case--the linear case was primarily a single frequency process.

All of the experimental results indicated that the nonlinear aspects of the combustion process were the dominant mechanisms controling combustion instability.

Both the closed-loop and twin-chambers analog technique of studying instability proved to be valuable methods for gaining insight into the phenomena being studied and both have potential for application to other similar problems.

The analytical work established a method for computing stability boundaries for velocity-sensitive combustion. It was established that the method used moderate amounts of computer time and predicted results that were in qualitative agreement with the known characteristics of velocity-sensitive combustion instability. The results of the numerical work were substantiated by comparison of approximate solutions obtained by perturbation procedures. In some cases, the perturbation solutions were obtained in closed form. It is felt that these explicit solutions are very helpful in understanding the physical nature of velocity-sensitive combustion instability.

REFERENCES

1. Priem, R. J. and Heidmann, M. F. "Propellant Vaporization as a Design Criterion for Rocket-Engine Combustion Chambers, "TR R-67, NASA, 1960.

2. Heidmann, M. F. "Amplification by Wave Distortion in Unstable Combustors," AIAA Journal, Vol. 9, February 1971, pp. 336-339.

3. Heidmann, M. F. "Amplification by Wave Distortion of the Dynamic Response of Vaporization Limited Combustion," TN D-6287, NASA, May 1971.

* 4. Hribar, A. E. "An Investigation of the Open-Loop Amplification of Reynolds Number Dependent Processes by Wave Distortion," an unsolicited Proposal for Research submitted to NASA, June 1971.

* 5. Ventrice, M. B. "An Investigation of the Open-Loop Amplification of a Reynolds Number Dependent Process by Wave Distortion," Ph.D. dissertation, Tennessee Technological University, June 1974.

* 6. Ventrice, M. B. and Purdy, K. R. "An Investigation of the Open-Loop Amplification of a Reynolds Number Dependent Process by Wave Distortion," CR-134620, NASA, May 1974.

* 7. Fang, J. C. and Purdy, K. R. "Calibration of a Constant-Temperature Hot-Wire Anemometer for Very Low Reynolds Numbers," Mechanical Engineering Report, ME-44, Tennessee Technological University, December 1973.

* 8. Fang, J. C. "On the Convection Limited Self-Sustained Acoustic Vibrations in a Closed-Closed Cylindrical Chamber," Ph.D. dissertation, Tennessee Technological University, August 1975.

* 9. Purdy, K. R., Ventrice, M. B., and Fang, J. C. "An Analytical Investigation of the Open-Loop Amplification of Reynolds Number Dependent Processes by Wave Distortion," Proceedings of the Tenth Southeastern Seminar on Thermal Sciences, April 1974, pp. 176-204.

10. Powell, E. A. "Nonlinear Combustion Instability in Liquid Propellant Rocket Engines," Ph.D. dissertation, Georgia Institute of Technology, 1970.

* 11. Ventrice, M. B., Purdy, K. R., and Fang, J. C. "Vaporization Limited Combustion Stability Study Using an Analog Process," 11th JANNAF Combustion Meeting Bulletin, (Chemical Propulsion Information Agency Publication 261), Vol. 2, December 1974, pp. 121-128.

12. Ventrice, M. B., Fang, J. C., and Purdy, K. R., "Amplification of Reynolds Number Dependent Processes by Wave Distortion," CR-134917, NASA, June 1975.

* 13. Purdy, K. R., Ventrice, M. B., and Fang, J. C. "The Important Ingredients for Self-Sustained Unsteady Combustion," 12th JANNAF Combustion Meeting Bulletin, (Chemical Propulsion Information Agency Publication 273), Vol. 2, December 1975, pp. 493-507.

* 14. Ventrice, M. B., Fang, J. C., and Purdy, K. R. "Simulation of Liquid Propellant Rocket Engine Combustion Instabilities," AIAA 17th Aerospace Sciences Meeting, Paper 79-0156, January 1979.

* 15. Ventrice, M. B., Fang, J. C., and Purdy, K. R., "Simulation of Liquid Propellant Rocket Engine Combustion Instabilities," AIAA Journal, to be published about December 1979.

16. Maslen, S. H. and Moore, F. K. "On Strong Transverse Waves Without Shocks in a Circular Cylinder," Journal of Aeronautical Sciences, Vol. 23, No. 6, 1956, pp. 525-538.

* 17. Ventrice, M. B. and Purdy, K. R. "Pressure and Velocity-Sensitive Feedback Mechanisms and Their Importance to Self-Sustained Unsteady Liquid Propellant Combustion," 13th JANNAF Combustion Meeting Bulletin (Chemical Propulsion Information Agency Publication 281), Vol. 3, December 1976, pp. 131-144.

* 18. Peddieson, Jr., J., Ventrice, M. B., and Purdy, K. R. "Effects of Nonlinear Combustion on the Stability of a Liquid Propellant System," 14th JANNAF Combustion Meeting Bulletin, (Chemical Propulsion Information Agency Publication 292), Vol. 1, December 1977, pp. 525-538.

* 19. Peddieson, Jr., J., Wong, K. W., and Ventrice, M. B., "Stability Boundaries for Velocity-Sensitive Unsteady Combustion Using the Galerkin and Collocation Methods," 15th JANNAF Combustion Meeting Bulletin, (Chemical Propulsion Information Agency Publication 297), Vol. 2, December 1978, pp. 461-472.

* 20. Wong, K. W. "Analysis of Combustion Instability in Liquid Fuel Rocket Motors," Ph.D. dissertation, Tennessee Technological University, August 1979.

* 21. Wong, K., Peddieson, Jr., J., and Ventrice, M. B. "Analysis of Combustion Instability in Liquid Fuel Rocket Motors," CR 159733, NASA, November 1979.

22. Nayfeh, A. H. Perturbation Methods, Pure and Applied Mathematics, A Wiley-Interscience Series of Texts, Monographs, and Tracts, 1972.

* 23. Googerdy, A. "Perturbation Solutions of Combustion Instability Problems," M.S. Thesis, Tennessee Technological University, June 1979.

* 24. Googerdy, A., Peddieson, Jr., J., and Ventrice, M. B. "Perturbation Solutions of Combustion Instability Problems," CR 159642, NASA, September 1979.

* 25. McDonald, G. H., "Stability Analysis of a Liquid Fuel Annular Combustion Chamber," M.S. Thesis, Tennessee Technological University, August 1979.

* 26. McDonald, G. H., Peddieson, Jr., J., and Ventrice M. B. "Stability Analysis of a Liquid Fuel Annular Combustion Chamber," CR 159734, NASA, November 1979.

All references marked with * are papers or reports which resulted from this research. In addition to the reports listed, semiannual reports were submitted every six months. Two of these semiannual reports, July through December 1973 and January through July 1975, were of special significance and were, therefore, assigned CR numbers. They are listed in the references as numbers 6 and 12. Also, informal reports were submitted on a somewhat monthly basis to the project's Technical Monitor, Dr. Richard J. Priem. These reports have some details in them that do not appear in the published work.

22 APR 1980

L. Scruggs 313/2715/32750 12/11/92